Alterations in the innate and adaptive immune system in a real-world cohort of multiple sclerosis patients treated with ocrelizumab

L. Beckers [a,b,1], P. Baeten [a,b,1], V. Popescu [a,b,c], D. Swinnen [a,b,d], A. Cardilli [a,b,d], I. Hamad [a,b,d], B. Van Wijmeersch [a,b,c], S.J. Tavernier [e,f], M. Kleinewietfeld [a,b,d,2], B. Broux [a,b,2], J. Fraussen [a,b,2], V. Somers [a,b,*,2]

[a] *University MS Center (UMSC), Hasselt-Pelt, Hasselt, Belgium*
[b] *Department of Immunology and Infection, Biomedical Research Institute, Hasselt University, Hasselt, Belgium*
[c] *Noorderhart, Rehabilitation and MS Center, Pelt, Belgium*
[d] *VIB Laboratory of Translational Immunomodulation, Center for Inflammation Research (IRC), Diepenbeek, Belgium*
[e] *Department of Internal Medicine and Pediatrics, Ghent University, Ghent, Belgium*
[f] *Unit of Molecular Signal Transduction in Inflammation, VIB-UGent Center for Inflammation Research (IRC), Ghent, Belgium*

ARTICLE INFO

ABSTRACT

B cell depletion by the anti-CD20 antibody ocrelizumab is effective in relapsing-remitting (RR) and primary progressive (PP) multiple sclerosis (MS). We investigated immunological changes in peripheral blood of a real-world MS cohort after 6 and 12 months of ocrelizumab.

All RRMS and most PPMS patients (15/20) showed treatment response. Ocrelizumab not only reduced CD20$^+$ B cells, but also numbers of CD20$^+$ T cells. Absolute numbers of monocytes, dendritic cells and CD8$^+$ T cells were increased, while CD56^{hi} natural killer cells were reduced after ocrelizumab. The residual B cell population shifted towards transitional and activated, IgA$^+$ switched memory B cells, double negative B cells, and antibody-secreting cells. Delaying the treatment interval by 2–3 months increased mean B cell frequencies and enhanced naive B cell repopulation. Ocrelizumab reduced plasma levels of interleukin(IL)-12p70 and interferon (IFN)-α2.

These findings will contribute to understanding ineffective treatment responses, dealing with life-threatening infections and further unravelling MS pathogenesis.

1. Introduction

Multiple sclerosis (MS) is one of the most common chronic inflammatory, demyelinating diseases of the CNS in young adults. In 85–90% of MS patients, the disease initiates as relapsing-remitting (RR)MS, characterized by alternating periods of clinical relapses and remission [1]. Over time, 15–30% of RRMS patients develops secondary progressive (SP)MS. In primary progressive (PP)MS (10–15% of MS patients), gradual clinical deterioration occurs from disease onset [1]. B cells contribute to MS pathogenesis, both by differentiation into antibody-secreting cells [2] and antibody-independent functions such as antigen presentation [3], costimulation [3], and cytokine production [4,5]. The

importance of B cell mediated pathology in MS has been emphasized by the clinical success of B cell depletion therapy in the treatment of RRMS and even PPMS patients [6,7].

Anti-CD20 B cell depleting monoclonal antibodies have been explored in several autoimmune and autoantibody-mediated diseases [8–11]. In MS, the chimeric rituximab, humanized ocrelizumab and recombinant human ofatumumab demonstrated a high efficacy for the treatment of RRMS [6,7,12]. Importantly, ocrelizumab was the first immunosuppressive agent reaching the primary endpoint in a clinical trial for early PPMS [7]. Therefore, it was licensed for the treatment of RRMS and PPMS by the US Food and Drug Administration in 2017. The phase 3 clinical trials for RRMS (OPERA I/II) and PPMS (ORATORIO) revealed that intravenous admission of 600 mg ocrelizumab every 24 weeks resulted in a decline of circulating B cells to negligible levels by week 2 until the end of follow-up (96 and 216 weeks, respectively) [6,7].

As CD20 is not expressed on antibody-secreting cells, the clinical effects of anti-CD20 therapy are due to antibody-independent mechanisms. However, long-term B cell depletion was recently associated with decreased serum immunoglobulin (Ig) levels, increasing the risk of (serious) infections [13,14]. In this light, MS patients on rituximab or ocrelizumab treatment showed an increased risk of severe COVID-19 infection with higher probabilities of hospitalization, admission to the intensive care unit and death [15–17]. Therefore, there is still a need for detailed profiling of changes in the immune system after B cell depletion therapy to better understand how B cell depletion impairs host defense against (life-threatening) infections. Additionally, insights into the lack of treatment response in a proportion of MS patients is still missing [18,19]. This study aimed to longitudinally investigate a real-world cohort of RRMS and PPMS patients followed up to one year after ocrelizumab initiation. Blood samples were collected before and after 6 and 12 months (M) of ocrelizumab treatment and used for in-depth immunological phenotyping of both the innate (monocytes, natural killer (NK) cells, dendritic cells (DCs)) and adaptive immune system (B and T cell subsets). In addition, an extensive characterization of the systemic cytokine profile was done before and during ocrelizumab treatment.

2. Methods

2.1. Human participants

Peripheral blood samples were obtained from 20 healthy controls (HC), 16 RRMS and 20 PPMS patients at the University Biobank Limburg (UBiLim; Hasselt, Belgium) [20] and Noorderhart hospital (Pelt, Belgium). MS patients were diagnosed according to the McDonald criteria [21]. This study was approved by the Committee of Medical Ethics from Hasselt University and Noorderhart. Written informed consent was obtained from all participants. Blood samples were collected from MS patients at the start of ocrelizumab (Ocrevus) treatment ($n = 15$ RRMS, $n = 18$ PPMS) and at the second (6 M; $n = 13$ RRMS, $n = 17$ PPMS) and third (12 M; $n = 12$ RRMS, n = 12 PPMS) infusion. Missing time points/data were due to organizational issues or patient withdrawal. For two RRMS patients, blood samples were additionally collected after a 2 M or 3 M treatment delay due to the COVID-19 pandemic ("restart"). All samples were cryopreserved at UBiLim. Donor characteristics are provided in Tables 1 and S1. HC did not have allergies, autoimmune disorders or infections at sampling and were matched to MS patients with regard to age and sex as closely as possible.

2.2. Flow cytometry

Peripheral blood mononuclear cells (PBMCs) were obtained via ficoll density gradient centrifugation (Cederlane lympholyte, Sheffield, UK) and frozen in liquid nitrogen. At the time of analysis, samples were thawed and rested for 2 h at 37 °C, 5% CO_2. After live/dead staining using Fixable Viability Dye eFluor 506 (Thermo Fisher Scientific, Waltham, USA) or Zombie Aqua (BioLegend, San Diego, USA), samples were

Table 1
Baseline donor clinical characteristics.

	MS		HC
	RRMS	PPMS	
Number of donors	16	20	20
Start ocrelizumab	15	18	NA
6 M ocrelizumab	13	17	NA
12 M ocrelizumab	12	12	NA
Restart ocrelizumab	2	0	NA
Age at baseline[a]	42.0 (21.0–62.0)	49.5 (28.0–70.0)	48.0 (26.0–67.0)
Sex, % F	80	30	50
Disease duration since MS diagnosis[a]	10.0 (1.0–29.3)	3.9 (0.3–20.0)	NA
Last treatment before ocrelizumab[b]			
Untreated	1	7	NA
Interferon beta-1a	2	0	
Teriflunomide	1	3	
Glatiramer acetate	0	1	
Dimethyl fumarate	4	3	
Fingolimod	3	0	
Natalizumab	4	0	
Cyclophosphamide	1	6	
EDSS at baseline[b]	2.5 (0.0–6.0)	4.5 (1.0–6.5)	NA
EDSS deterioration during ocrelizumab treatment[c]	0 of 14 (0%)	4 of 17 (22.5%)[d]	
Number of T2 lesions on MRI[c]			
< 10 lesions	1 of 15 (6.7%)	4 of 19 (21.1%)	NA
10–50 lesions	11 of 15 (73.3%)	11 of 19 (57.9%)	
50–100 lesions	3 of 15 (20.0%)	4 of 19 (21.1%)	
Change of MRI activity during ocrelizumab treatment	↑: 0 ↓: 0	↑: 1 ↓: 0	
Patients showing Gd+ lesions[c]	6 of 15 (40%)	3 of 20 (15.0%)	NA
Change of MRI activity during ocrelizumab treatment	↑: 0 ↓: 5	↑: 0 ↓: 2	
Patients with relapses after ocrelizumab initiation	0	0	NA
Patients with NEDA-3 after 12 M ocrelizumab treatment[c]	15 of 15 (100%)	15 of 20 (75%)	NA
Patients with hypogammaglobulinemia[c]	3 of 15 (20%)	3 of 17 (17.6%)	NA
Patients that switched to other treatment during study period	0	0	NA

Abbreviations: EDSS, expanded disability status scale; F, female; Gd+, gadolinium-enhancing lesions; M, months; MRI, magnetic resonance imaging; NA, not applicable; NEDA-3, no evidence of disease activity = no disability progression, no relapse, no new or newly enlarged T2 lesions and no Gd+ lesions.
[a] In years, median (range).
[b] Data available for n = 15 RRMS and $n = 18$ PPMS, median (range).
[c] n (%).
[d] 2 PPMS patients showed EDSS deterioration after 6 M and 2 PPMS patients after 12 M of ocrelizumab treatment.

stained with three different antibody panels to analyze general immune cells, B and T cell subsets (Table S2). The isotypes IgG, IgA and IgM were stained on B cells using a surface staining. PBMCs were fixed (CytoFix Fixation Buffer, BD Biosciences, Erembodegem, Belgium) or permeabilized using the FOXP3/Transcription factor staining buffer kit (Thermo Fisher Scientific) according to the manufacturer's instructions. Human TruStain FcX and True-Stain Monocyte Blocker (BioLegend) were also used. Samples were acquired using the FACSymphony or LSRFortessa (BD Biosciences) and analyzed using FlowJo 10.8.0 (BD Biosciences) and FlowSOM [22]. For manual gating, fluorescence minus one controls were used. The gating strategy is depicted in Figs. S1 and S2. To avoid inter-assay variation, all samples of the same donor were processed simultaneously. Absolute lymphocyte and monocyte numbers were obtained from standard clinical lab tests performed before ($n = 14$ RRMS, $n = 18$ PPMS), 6 M ($n = 13$ RRMS, $n = 16$ PPMS) and 12 M ($n =$

12 RRMS, n = 12 PPMS) after ocrelizumab initiation. Absolute number of immune cell subsets was calculated as follows: absolute lymphocyte or monocyte number (/μl) X percentage of lymphocyte or monocyte subset.

2.3. FlowSOM analysis

Flow cytometry data were manually gated to single live cells and exported to FlowJo 10.8.0. Only MS patients with available blood samples at all three time points (before, 6 M and 12 M after ocrelizumab) were included (n = 10 RRMS, n = 11 PPMS) along with age-and-sex-matched HC (n = 9). Analysis was performed using the FlowSOM algorithm [22]. All data were concatenated, scaled, and log-transformed on import. Cells were assigned to a Self-Organizing Map (SOM) with a 16×16 grid, grouping similar cells into 256 nodes. Each node in the FlowSOM tree was assigned to a score indicating its correspondence to the desired cell profile. A minimal spanning tree was constructed to visualize similar nodes in branches. Cell numbers were scaled logarithmically and nodes with similar expression markers were clustered into metaclusters. The FlowSOM algorithm was run at least three times to ensure reproducibility. Comparisons between time points were performed with Friedman test and a Benjamini-Hochberg corrected test by calculating the mean percentage per sample group in each cluster and testing statistical significance for each node within metaclusters. P-values were two-sided and analysis was performed using RStudio (Version 1.4.1106). Significant differences were defined by $p < 0.05$.

2.4. Bead-based immunoassay

Plasma samples were collected from MS patients before (n = 15 RRMS, n = 18 PPMS), 6 M (n = 13 RRMS, n = 17 PPMS) and 12 M (n = 12 RRMS, n = 12 PPMS) after start of ocrelizumab treatment and immediately stored at −80 °C. The LEGENDplex™ Human Anti-Virus Response Panel kit (BioLegend) was used to measure circulating concentrations of tumor necrosis factor (TNF)-α, interleukin (IL)-1β, IL-8, IL-6, interferon gamma-induced protein (IP)-10, granulocyte-macrophage colony-stimulating factor (GM-CSF), IL-12, interferon (IFN)-α, IFN-β, IFN-γ, IFN-λ1, IFN-λ2/3 and IL-10. The kit was used according to the manufacturer's instructions with minor adjustments. The assay was carried out in V-bottom 96-well plates and 12.5 μl of plasma samples and reagents were added. All plasma samples were diluted twofold with assay buffer and tested in duplicate. Samples were acquired using the LSRFortessa (BD Biosciences) and analyzed using LEGENDplex™ Data Analysis Software Suite (BioLegend). Means of detection limits of duplicate tests were calculated and were used as a reference for cytokine levels under the detection limit.

2.5. Statistical analysis

Data analysis was done using Prism software version 9.5 (GraphPad Software, San Diego, CA, USA) and SAS JMP Pro 16 software (SAS Institute, Cary, NC, USA). Differences in immune cell subsets between start, 6 M and 12 M of ocrelizumab treatment were assessed by a linear mixed model with random effects (sample ID) and fixed effects (age, sex, timepoint, expanded disability status scale (EDSS), disease duration, previous treatments and all interactions with timepoint), allowing for repeated measurements and missing values. The most common confounders were age, sex and EDSS. Normality was checked using a normal quantile plot of the conditional residuals of the model and if needed, the data was log-transformed. To determine whether group means differed, pairwise comparisons were conducted using the Tukey post-hoc test. Differences between HC and MS samples at ocrelizumab initiation were analyzed using the Mann-Whitney test. A $p < 0.05$ was considered significant.

3. Results

3.1. Demographic and clinical characteristics

Peripheral blood samples were collected from 20 HC, and 16 RRMS and 20 PPMS patients before, 6 M and 12 M after ocrelizumab initiation (Table 1). In this real-world patient cohort, most RRMS (15/16, 93.8%) and PPMS (13/20, 65%) patients had received other disease modifying therapies before ocrelizumab treatment (Table S1). No evidence of disease activity (NEDA) was defined according to the 3 parameter NEDA (NEDA-3): no disease progression (measured by EDSS), no new clinical relapse and absence of new or newly enlarged T2 lesions and gadolinium-enhancing (Gd+) lesions [23]. All RRMS patients reached NEDA-3 during the observation period, whereas 5/20 (25%) PPMS patients did not. Of these non-responding PPMS patients, four experienced a deterioration in EDSS and one developed a new T2 lesion during ocrelizumab treatment. None of the RRMS and PPMS patients experienced a clinical relapse or switched to another treatment during the study period.

3.2. High-dimensional immune profiling shows a CD20+ cell-specific depletion by ocrelizumab

B cells were efficiently depleted following ocrelizumab treatment, with CD20+ B cell numbers significantly reduced in both RRMS and PPMS patients at 6 M (96% and 98%, respectively) and 12 M (98% and 94%, respectively; Table 2). CD20+ cells within the T cell population were also significantly decreased by ocrelizumab. Although total CD3+ T cell numbers remained unchanged, the absolute number of CD8+ T cells was significantly increased in PPMS patients at 12 M of ocrelizumab treatment. Within the innate immune cell population, the absolute number of CD56hi NK cells was significantly reduced at 6 M of ocrelizumab treatment in RRMS but not in PPMS patients. The absolute number of DCs was not altered in RRMS patients, but was significantly increased at 6 M of ocrelizumab treatment in PPMS patients. At 12 M of ocrelizumab treatment, a significant increase in the number of myeloid DCs (mDCs) and plasmacytoid DCs (pDCs) in RRMS patients and of mDCs in PPMS patients was found (Table S3). Furthermore, the absolute number of monocytes was significantly increased at 6 M and 12 M of ocrelizumab treatment in RRMS patients and at 12 M in PPMS patients. Within the monocyte population, the absolute number of CD14+ monocytes was increased at 12 M in PPMS patients (Table S3). In summary, ocrelizumab treatment reduced CD20+ immune cells and CD56hi NK cells, but increased CD8+ T cells, monocytes and DCs.

The effect of ocrelizumab treatment on the frequencies of immune cell subsets was additionally investigated using unbiased clustering by FlowSOM analysis [22,24]. An overlay of the manually gated data on the FlowSOM tree indicated separate clustering of the major immune cell subsets (Figs. 1A, S3, S4). Confirming the manual analysis, all B cell clusters were significantly decreased following ocrelizumab treatment in both RRMS and PPMS patients (Fig. 1B-C), except for two nodes at 6 M in both patient groups (1, 2, Fig. 1B-C) and one node at 12 M in PPMS patients (3, Fig. 1C). Node 1 was defined as CD20+IgD+CD27−CD24+CD38highCXCR5+, node 2 as CD20+IgD+CD27−CD24+CD38highCXCR5− and node 3 as CD20+IgD+CD27−CD24+CD38+CXCR5+, partially overlapping with transitional B cells. No significant differences were found between the 6 M and 12 M time points and between start and HC (data not shown) in both RRMS and PPMS patients. Furthermore, no significant changes were observed in the other immune cell subsets. To ensure that rare subpopulations of CD4+ T cells are captured with our analyses, CD4+ T helper (Th) cell subsets were studied in more detail by FlowSOM analysis (Figs. S5, S6). However, no significant results were observed, confirming that B cells are the main immune cell subset targeted and changed by ocrelizumab treatment in our real-world cohort.

Table 2

Changes in the absolute number (cells/μl) of innate and adaptive immune cells before and after start of ocrelizumab treatment in RRMS and PPMS patients.

	START Mean ± SEM	6 M Mean ± SEM	p-value 6 M vs START	12 M Mean ± SEM	p-value 12 M vs START 12 M vs 6 M
RRMS					
CD20$^+$ B cells	372.37 ± 88.11	14.27 ± 8.20	**p < 0.0001**	6.62 ± 5.52	**p < 0.0001**
CD3$^+$ T cells	987.47 ± 182.37	818.13 ± 140.82	p = 0.2251	932.72 ± 147.14	p = 0.9112
CD3$^+$CD20$^+$ T cells	0.55 ± 0.12	0.11 ± 0.03	**p < 0.0001**	0.19 ± 0.07	**p = 0.0006**
CD3$^+$CD4$^+$ T cells	609.16 ± 126.82	527.16 ± 102.0	p = 0.1003	612.13 ± 102.06	p = 0.9393
CD3$^+$CD8$^+$ T cells	278.47 ± 49.74	216.41 ± 33.16	p = 0.1709	246.38 ± 35.09	p = 0.567
NK cells	237.23 ± 31.04	204.80 ± 25.93	p = 0.4103	207.94 ± 32.09	p = 0.8255
DCs	225.90 ± 14.79	258.68 ± 16.11	p = 0.4898	275.58 ± 32.10	p = 0.1177
Monocytes	144.33 ± 14.74	196.53 ± 26.43	**p = 0.0137**	221.42 ± 28.86	**p < 0.0001** **p = 0.0347**
PPMS					
CD20$^+$ B cells	266.17 ± 38.49	5.16 ± 3.57	**p < 0.0001**	15.5 ± 10.84	**p < 0.0001**
CD3$^+$ T cells	937.89 ± 91.04	1134.17 ± 127.16	p = 0.2591	1057.19 ± 101.98	p = 0.23
CD3$^+$CD20$^+$ T cells	0.45 ± 0.08	0.08 ± 0.2	**p = 0.0002**	0.15 ± 0.06	**p = 0.001**
CD3$^+$CD4$^+$ T cells	597.87 ± 72.06	743.21 ± 110.42	p = 0.2042	683.1 ± 58.60	p = 0.2989
CD3$^+$CD8$^+$ T cells	267.63 ± 29.08	307.75 ± 32.52	p = 0.9053	287.79 ± 42.41	**p = 0.0076** **p = 0.0241**
NK cells	195.37 ± 22.74	247.10 ± 36.91	p = 0.1115	270.49 ± 36.42	p = 0.1237
DCs	257.89 ± 23.42	291.47 ± 28.20	**p = 0.0049**	340.54 ± 48.89	p = 0.0807
Monocytes	166.36 ± 14.73	184.92 ± 19.27	p = 0.7504	270.03 ± 27.57	**p = 0.0031** **p = 0.0232**

Absolute number (cells/μl) of immune cell subsets in the peripheral blood of RRMS and PPMS patients before (i.e. start, n = 14 and n = 18, respectively), at 6 M (n = 13 and n = 16, respectively) and at 12 M (n = 12 each) of ocrelizumab treatment. NK cells were defined as CD3$^-$CD56$^+$, DCs as CD3$^-$CD56$^-$CD20$^-$HLADR$^+$CD14$^-$CD27$^-$ and monocytes as CD3$^-$CD56$^-$CD20$^-$HLADR$^+$CD14$^+$. Mean with SEM are shown. *P*-values in bold are statistically significant. Differences in the immune cell subsets were assessed by a linear mixed model and normal distribution was checked using a normal quantile plot of the conditional residuals of the model. Abbreviations: DCs, dendritic cells; NK, natural killer cells; SEM, standard error of the mean.

3.3. Ocrelizumab induces a shift in the distribution of residual B cell subsets

The B cell population was investigated in more detail by analysis of CD24^{high}CD38^{high} transitional B cells, IgD$^+$CD27$^-$ naive B cells, IgD$^+$CD27$^+$ unswitched memory B cells, IgD$^-$CD27$^+$ switched memory B cells, IgD$^-$CD27$^-$ double negative B cells and CD27^{high}CD38^{high} antibody-secreting cells. In addition, the transitional B cell population was divided into CD21$^-$ transitional (T)1 and CD21$^+$ T2 transitional B cells, while naive B cells were separated in CD21$^-$ activated naive and CD21$^+$ resting naive B cells. Switched memory B cells comprised both IgM-only and IgG$^+$, IgA$^+$ or IgE$^+$ B cells. Within double negative B cells,

CD21$^-$ and CD21$^+$ double negative B cells were discriminated. For both RRMS and PPMS patients, the absolute number of all B cell subsets was significantly decreased after 12 M of ocrelizumab, except for T2 transitional B cells in RRMS patients and T1 transitional B cells in PPMS patients (Table S4).

Moreover, the frequency of total B cells was significantly decreased in RRMS and PPMS patients at 6 M (92% and 94%, respectively) and 12 M (96% and 93%, respectively) of ocrelizumab treatment compared to start (Figs. 2, S7, respectively; *p*-values in Table S5). Within the residual B cell population, ocrelizumab induced a shift towards significantly more transitional, switched memory and double negative B cells and antibody-secreting cells in all MS patients after 6 M and 12 M of ocrelizumab treatment (Figs. 2, S7, Table S5). In contrast, frequencies of naive and unswitched memory B cells were significantly decreased following ocrelizumab treatment in RRMS and PPMS patients. Within the transitional B cell population, ocrelizumab treatment resulted in a shift towards more T1 transitional B cells and fewer T2 transitional B cells, while naive B cells shifted towards more activated naive and fewer resting naive B cells in both patient groups. Additionally, there was an increase in CD21$^-$ cells and a decrease in CD21$^+$ cells in the double negative B cell population. Interestingly, the frequency of double negative B cells was significantly increased in PPMS patients who did not reach NEDA-3 (*n* = 4) compared to PPMS patients who reached NEDA-3 after 12 M of ocrelizumab treatment (*n* = 8, *p* = 0.0283, Fig. S8). At baseline, the total B cell population was increased while unswitched memory B cells were slightly decreased in both RRMS (*p* = 0.0119 and *p* = 0.0556, respectively, Fig. 2) and PPMS patients (*p* = 0.0149 and *p* = 0.0548, respectively, Fig. S7) compared to HC. Thus, although the total B cell population was depleted after ocrelizumab treatment, a shift in the distribution of the residual B cell subsets was observed towards T1 transitional, switched memory and double negative B cells, and antibody-secreting cells.

3.4. The residual B cell population mainly consists of activated IgA$^+$ B cells

The phenotype of the residual antigen-experienced B cell subsets after ocrelizumab treatment (antibody-secreting cells, switched memory and double negative B cells) was studied by measuring their expression of the activation markers CD86 and CD80 and Ig isotypes (IgM, IgG, IgA) (Figs. 3, S9). Samples of ocrelizumab treated patients with <10 acquired B cells following analysis were excluded. The frequency of CD86$^+$ cells was significantly increased after ocrelizumab treatment within the remaining switched memory and double negative B cells of all patients, and in the antibody-secreting cells of RRMS patients (*p*-values in Table S6). Additionally, the frequency of CD80$^+$ cells was significantly higher in both switched memory and double negative B cells following ocrelizumab treatment. In contrast, CD80$^+$ cell frequencies were decreased in antibody-secreting cells of PPMS patients at 6 M of ocrelizumab. For the Ig isotypes, a shift was observed towards more IgA$^+$ and less IgG$^+$ cells within antibody-secreting cells, switched memory and double negative B cells of all patients at both timepoints. To conclude, ocrelizumab treatment induced a shift in the phenotype of the residual antigen-experienced B cells towards an activated (CD86 and CD80 expression) and IgA class-switched phenotype.

3.5. Increasing the time between two doses of ocrelizumab could result in a repopulation of early B cell subsets

During the COVID-19 pandemic, blood samples were collected of two RRMS patients whose time to the next dose (i.e. 18 M timepoint) was delayed by either 2 M (RRMS2) or 3 M (RRMS3), resulting in a time interval of 8 M or 9 M between the third and fourth dose. To study the impact of the extended interval between ocrelizumab doses on B cell frequencies and subset distribution within these two patients, we performed an in-depth B cell phenotypic analysis (Fig. 4). Although no
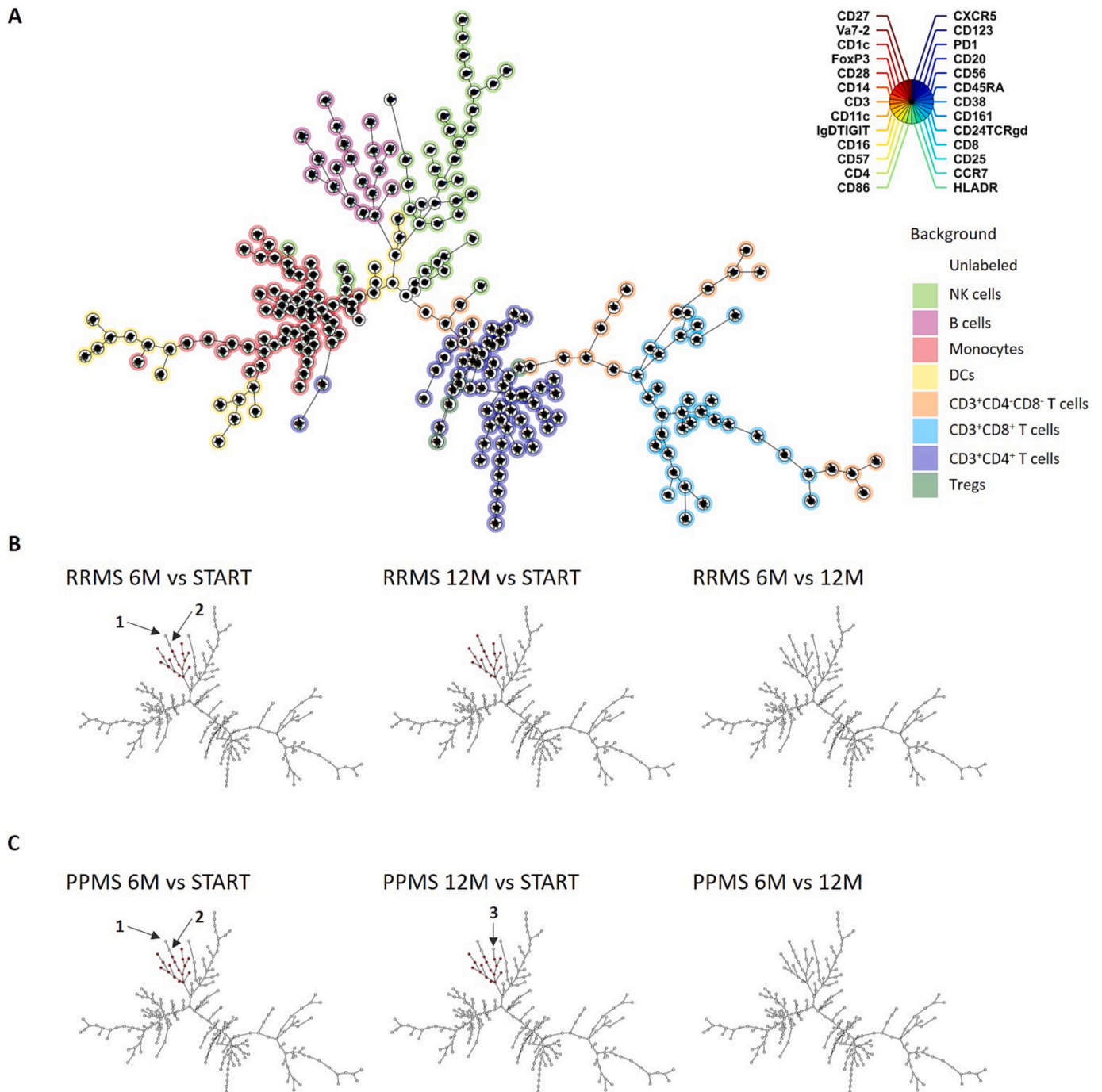
Fig. 1. Distribution of the major immune cell subsets after ocrelizumab treatment in RRMS and PPMS patients. A. FlowSOM tree (16×16) with the main immune cell subsets within single live cells (based on manual gating). Only MS patients with available blood samples at all three time points (before, 6 M and 12 M after ocrelizumab) were included ($n = 10$ RRMS, $n = 11$ PPMS) along with age-and sex-matched HC ($n = 9$). Each subset is colored as shown in the legend. Immune cell subsets were identified using manual gating: $CD3^-CD56^-CD20^-HLADR^+CD14^+$ monocytes, $CD3^-CD56^-CD20^-HLADR^+CD14^-CD27^-$ DCs, $CD3^-CD56^-CD20^+$ B cells, $CD3^-CD56^+$ NK cells, $CD8^+$ cytotoxic and $CD4^+$ helper T (Th) cells, with $CD25^+FOXP3^+$ regulatory T cells (Treg) as part of the $CD4^+$ T cells. Node sizes are equalized (relative node sizes in Figs. S1, S2). Nodes are built out of different markers as represented by the starchart legend. Comparison of start versus 6 M, start versus 12 M and 6 M versus 12 M of ocrelizumab treatment for RRMS (B) and PPMS (C) patients. Node 1 is defined as $CD20^+IgD^+CD27^-CD24^+CD38^{high}CXCR5^+$, node 2 as $CD20^+IgD^+CD27^-CD24^+CD38^{high}CXCR5^-$ and node 3 as $CD20^+IgD^+CD27^-CD24^+CD38^+CXCR5^+$. Comparisons between time points were performed using a Benjamini-Hochberg corrected test. Nodes significantly decreased compared to start are indicated in red. Abbreviations: DCs, dendritic cells; M, month; NK, natural killer cells; Treg: regulatory T cell. (For interpretation of the references to colour in this figure legend, the reader is referred to the web version of this article.)

statistical analysis could be performed, the total B cell frequency was increased with delayed ocrelizumab treatment in both RRMS patients, indicating B cell repopulation. Still, the B cell frequency was lower than at treatment initiation. Delayed ocrelizumab treatment further allowed a repopulation of naive B cells whereas the proportion of antibody-secreting cells, switched memory and double negative B cells was decreased. Additionally, the ocrelizumab-induced shift in transitional and naive B cell subsets was now reversed from activated naive towards resting naive B cells and T1 transitional towards T2 transitional B cells. The remaining antibody-secreting cells, switched memory and double
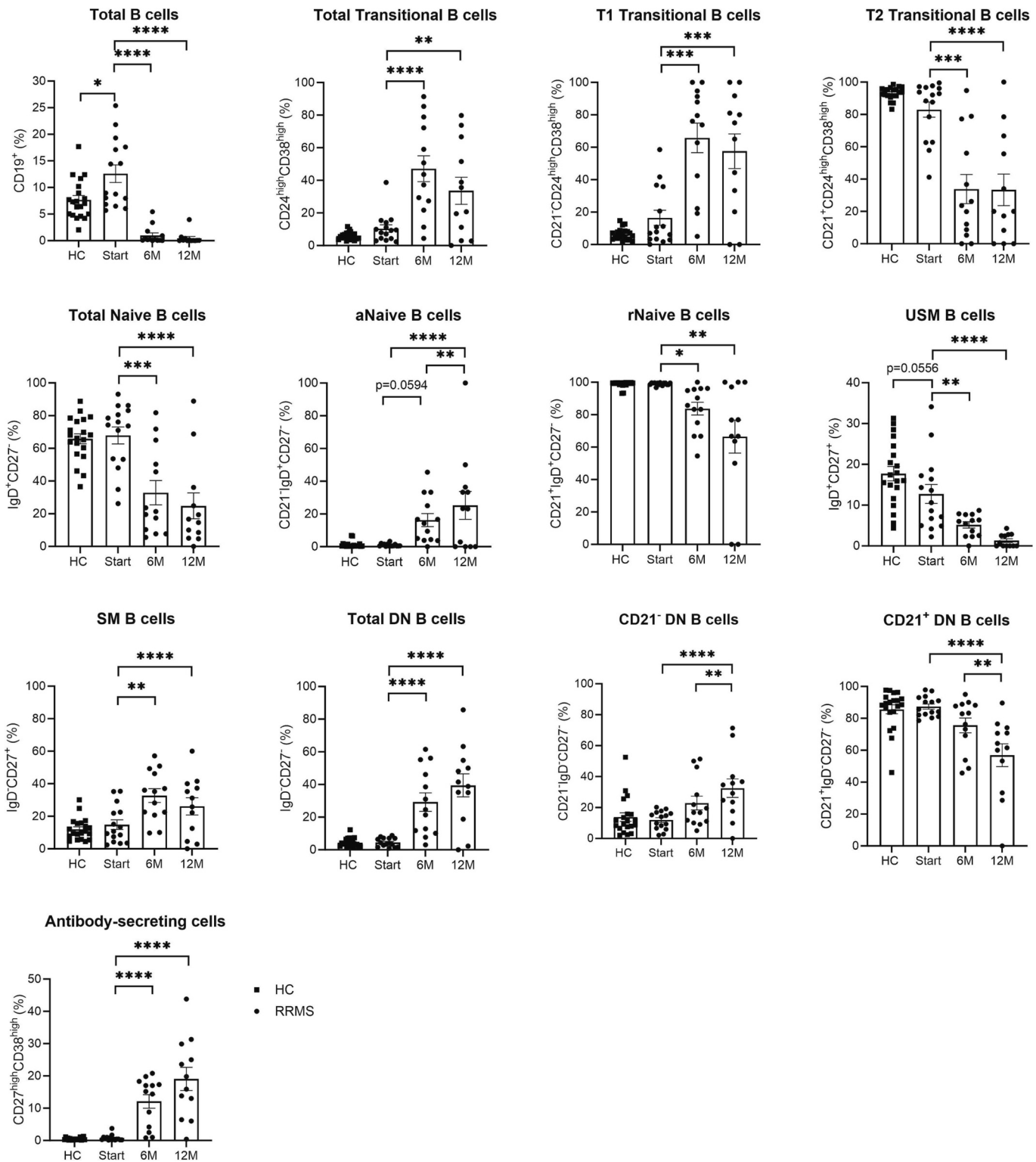
Fig. 2. Distribution of B cell subsets in HC and before and after start of ocrelizumab treatment in RRMS patients. Frequency of B cell subsets in the peripheral blood of 20 HC and 16 RRMS patients before (i.e. start, $n = 15$) after 6 M ($n = 13$) and 12 M ($n = 12$) of ocrelizumab treatment. B cell subsets are gated within the total $CD19^+$ B cell population. Percentages of total $CD19^+$ B cells, $CD24^{high}CD38^{high}$ transitional B cells, $CD21^-$ transitional (T1) B cells, $CD21^+$ transitional (T2) B cells, IgD^+CD27^- naive B cells, $CD21^-$ aNaive B cells, $CD21^+$ rNaive B cells, IgD^+CD27^+ USM B cells, IgD^-CD27^+ SM B cells, IgD^-CD27^- DN B cells, $CD21^-$ DN B cells, $CD21^+$ DN B cells and antibody-secreting cells are depicted. Mean $\pm$ SEM are shown. *$p < 0.05$, **$p < 0.01$, ***$p < 0.001$, ****$p < 0.0001$. Differences in B cell subsets were assessed by a linear mixed model and normal distribution was checked using a normal quantile plot of the conditional residuals of the model. Differences between HC and MS samples at the start of ocrelizumab treatment were analyzed using the non-parametric Mann-Whitney test. Abbreviations: aNaive, activated Naive B cells; SM, switched memory; DN, double negative; M, month; USM, unswitched memory; rNaive, resting naive B cells; SEM, standard error of the mean.
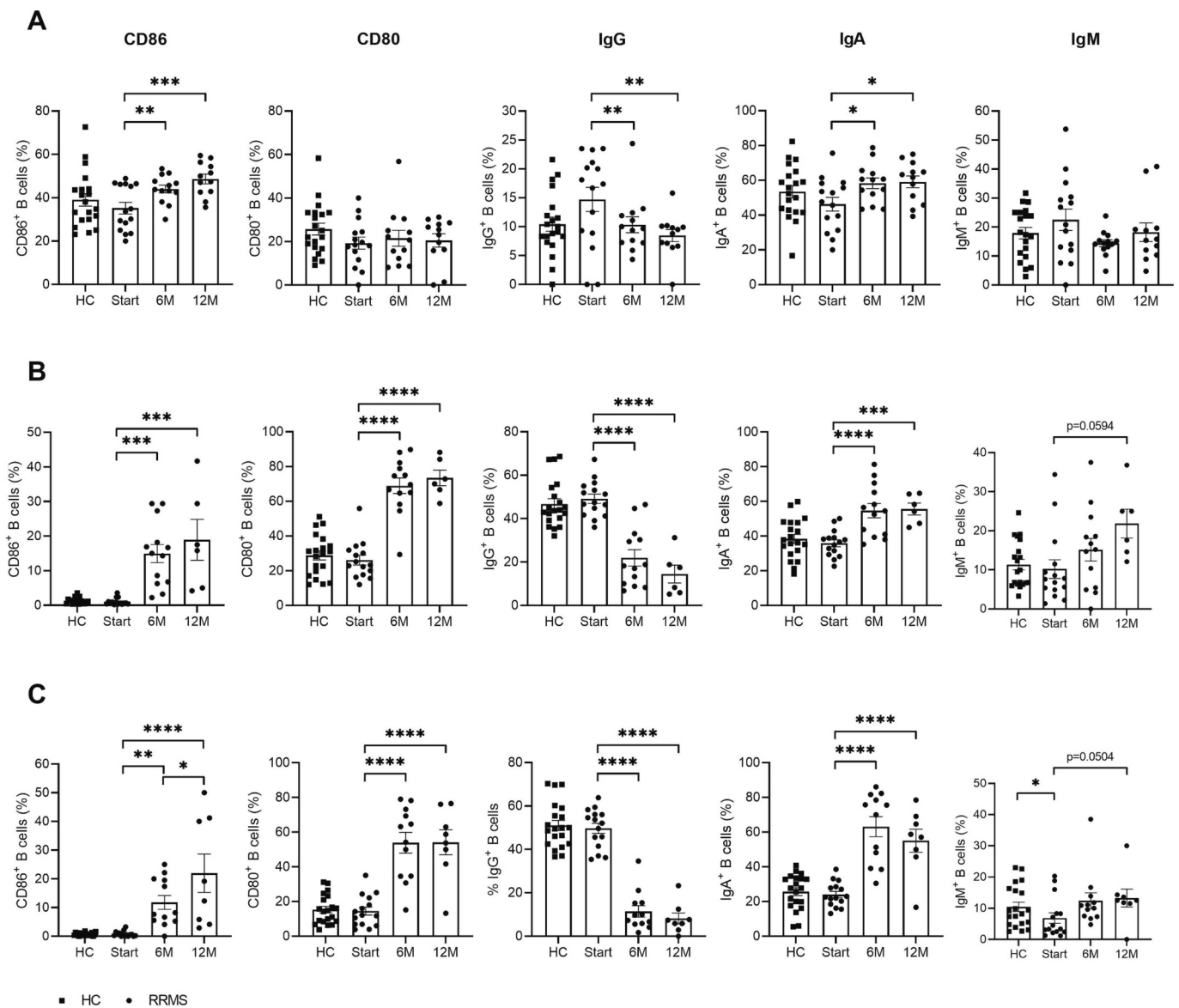
Fig. 3. Phenotypic characterization of the residual B cell subsets after ocrelizumab treatment in RRMS patients. Frequency of the activation markers CD86 and CD80 and the Ig isotypes IgG, IgA and IgM within antibody-secreting cells (A), SM B cells (B) and DN B cells (C) in the peripheral blood of 20 HC and 16 RRMS patients before (i.e. start), after 6 M and 12 M of ocrelizumab treatment was measured using flow cytometry. B cell subsets were gated within the total CD19$^+$ B cell population. Patient samples with <10 B cells left after ocrelizumab treatment were excluded from the analysis. All patient samples showed sufficient numbers of antibody-secreting cells after 6 M and 12 M of ocrelizumab treatment (start: $n = 15$, 6 M: $n = 13$, 12 M: $n = 12$), whereas 6 patients showed an insufficient number of SM B cells after 12 M of ocrelizumab treatment (start: n = 15, 6 M: n = 13, 12 M: $n = 6$). For the DN B cells, 1 patient showed an insufficient number of DN B cells after 6 M of ocrelizumab treatment and 4 patients after 12 M of ocrelizumab (start: n = 15, 6 M: n = 12, 12 M: $n = 8$). Mean ± SEM are shown. *p < 0.05, **p < 0.01, ***p < 0.001, ****p < 0.0001. Differences in the frequency of activation markers and Ig isotypes were assessed by a linear mixed model and normal distribution was checked using a normal quantile plot of the conditional residuals of the model. Differences between HC and MS samples at the start of ocrelizumab treatment were analyzed using the non-parametric Mann-Whitney test. Abbreviations: SM, switched memory; DN, double negative; M, month; SEM, standard error of the mean.

negative B cells showed a lower frequency of CD86$^+$ cells with delayed ocrelizumab dosing (Fig. S10). Nevertheless, the shift towards increased IgA$^+$ B cell frequencies and decreased IgG$^+$ B cell frequencies was still observed in switched memory and double negative B cells (Fig. S10). In conclusion, it is suggested that delaying the next ocrelizumab dose by 2 M or 3 M could lead to a repopulation of the antigen-inexperienced B cell populations and reduced expression of the activation marker CD86 in antigen-experienced cells.

3.6. Ocrelizumab treatment induces changes in plasma cytokine levels of RRMS and PPMS patients

Since the systemic cytokine profile of MS patients after ocrelizumab treatment is not completely understood, the concentration of 13 cytokines involved in inflammation and anti-viral immunity was measured in the plasma of RRMS and PPMS patients before ($n = 15$ and $n = 18$, respectively), after 6 M ($n = 13$ and $n = 17$, respectively) and 12 M ($n = 12$ each) of ocrelizumab treatment. IL-12p70 and IFN-α2 levels were significantly lower in all MS patients after 12 M of ocrelizumab treatment (Table 3). In PPMS patients, the concentration of IL-10 was significantly reduced after 12 M of ocrelizumab, whereas IL-8 was increased after 6 M and decreased again after 12 M (Table 3). All other cytokine levels were not significantly changed after ocrelizumab treatment. Remarkably, IFN-γ levels were significantly increased in PPMS patients who did not reach NEDA-3 ($n = 4$) compared to PPMS patients who reached NEDA-3 after 12 M of ocrelizumab treatment ($n = 8$, *p =*
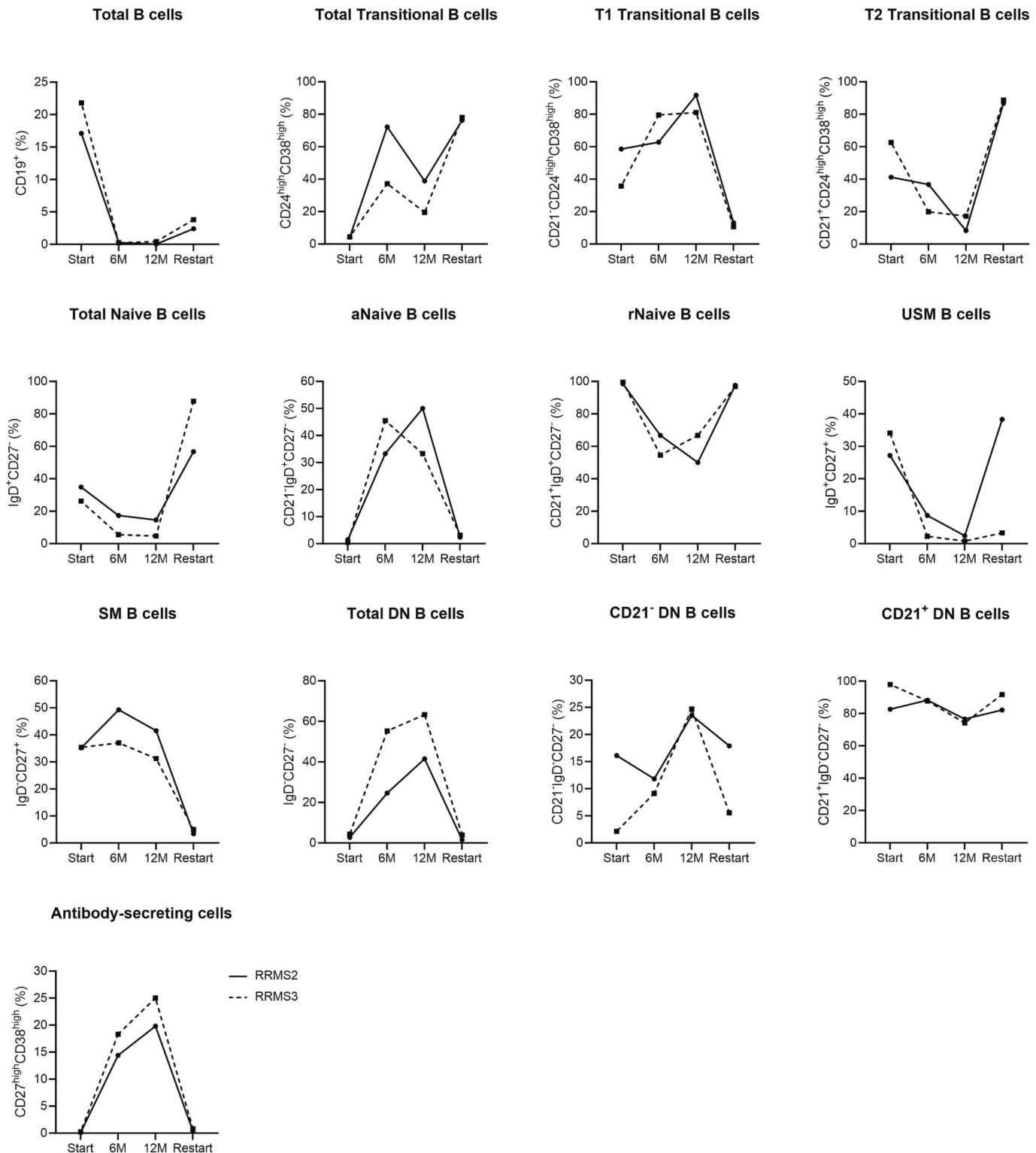
Fig. 4. Distribution of the B cell subsets after ocrelizumab treatment in two RRMS patients with an extended time to the next dose of ocrelizumab. Frequency of B cell subsets in the peripheral blood of 2 RRMS patients (RRMS2 and RRMS3) before (i.e. start), after 6 M, 12 M and 20 M (RRMS2) or 21 M (RRMS3) of ocrelizumab treatment. B cell subsets are gated within the total CD19$^+$ B cell population. Percentages of total CD19$^+$ B cells, CD24^{high}CD38^{high} transitional B cells, CD21$^-$ transitional (T1) B cells, CD21$^+$ transitional (T2) B cells, IgD$^+$CD27$^-$ naive B cells, CD21$^-$ aNaive B cells, CD21$^+$ rNaive B cells, IgD$^+$CD27$^+$ USM B cells, IgD$^-$CD27$^+$ SM B cells, IgD$^-$CD27$^-$ DN B cells, CD21$^-$ DN B cells, CD21$^+$ DN B cells, Antibody-secreting cells. Abbreviations: aNaive, activated Naive B cells; SM, switched memory; DN, double negative; M, month; USM, unswitched memory; rNaive, resting naive B cells.

Table 3
Circulating cytokine levels from RRMS and PPMS patients before and after start of ocrelizumab treatment.

	START	6 M		12 M	
	Mean ± SEM	Mean ± SEM	p-value 6 M vs START	Mean ± SEM	p-value 12 M vs START 12 M vs 6 M
RRMS					
IL-1β	5.54 ± 3.01	6.53 ± 2.45	p = 0.8703	2.98 ± 1.22	p = 0.5089
IL-6	3.91 ± 0.86	5.08 ± 2.16	p = 0.9608	8.98 ± 7.02	p = 0.5906
TNF-α	10.10 ± 2.78	8.10 ± 3.92	p = 0.3886	7.87 ± 2.86	p = 0.3917
IP-10	49.60 ± 3.58	57.29 ± 7.18	p = 0.2733	56.49 ± 7.83	p = 0.4938
IL-8	32.65 ± 24.94	4.65 ± 1.46	p = 0.4737	16.11 ± 8.04	p = 0.7782
IL-12p70	2.17 ± 0.36	1.69 ± 0.24	p = 0.1095	1.26 ± 0.09	**p = 0.0031**
IFN-γ	16.59 ± 2.37	12.53 ± 1.72	p = 0.4591	14.21 ± 3.06	p = 0.3475
GM-CSF	6.73 ± 1.35	5.87 ± 1.07	p = 0.5462	4.28 ± 0.24	p = 0.0926
IFN-λ1	37.47 ± 5.52	30.02 ± 4.63	p = 0.9923	23.78 ± 3.37	p = 0.5980
IFN-β	10.13 ± 2.85	9.22 ± 3.05	p = 0.9075	9.59 ± 3.30	p = 0.9624
IFN-α2	4.56 ± 1.37	3.52 ± 1.36	p = 0.9771	3.36 ± 1.53	**p = 0.0336**
IFN-λ2/3	95.32 ± 14.60	84.36 ± 14.33	p = 0.7651	72.63 ± 16.81	p = 0.1063
IL-10	4.65 ± 1.47	3.69 ± 0.95	p = 0.5477	2.89 ± 0.64	p = 0.2948
PPMS					
IL-1β	8.42 ± 2.57	8.74 ± 2.97	p = 0.8346	4.32 ± 1.18	p = 0.9649
IL-6	6.32 ± 2.26	9.87 ± 3.93	p = 0.937	5.70 ± 2.18	p = 0.1476
TNF-α	9.04 ± 2.09	11.77 ± 3.05	p = 0.7036	11.02 ± 2.50	p = 0.7019
IP-10	51.58 ± 5.09	56.20 ± 7.62	p = 0.4238	62.87 ± 7.92	p = 0.099
IL-8	26.54 ± 9.26	171.14 ± 124.02	**p = 0.0134**	38.15 ± 29.52	p = 0.9957 **p = 0.0411**
IL-12p70	2.93 ± 0.71	2.40 ± 0.48	p = 0.2636	2.07 ± 0.55	**p = 0.0340**
IFN-γ	16.21 ± 2.01	17.61 ± 2.87	p = 0.9810	19.25 ± 2.46	p = 0.6745
GM-CSF	10.44 ± 4.90	8.84 ± 3.07	p = 0.4640	7.49 ± 3.82	p = 0.1293
IFN-λ1	42.3 ± 5.26	44.59 ± 6.52	p = 0.9923	34.60 ± 6.04	p = 0.5980
IFN-β	24.80 ± 13.14	12.42 ± 5.62	p = 0.9075	13.19 ± 8.97	p = 0.9624
IFN-α2	5.03 ± 7.75	3.62 ± 1.01	p = 0.9771	2.40 ± 0.69	**p = 0.0336**
IFN-λ2/3	99.29 ± 13.87	89.04 ± 14.20	p = 0.7651	67.84 ± 6.26	p = 0.1063
IL-10	4.19 ± 0.99	3.73 ± 0.95	p = 0.5016	2.53 ± 0.91	**p = 0.0271**

Cytokine concentration (pg/ml) in plasma of RRMS and PPMS patients before (i.e. start; n = 15 and n = 17, respectively), after 6 M (n = 13 and n = 17, respectively) and 12 M (n = 12 each) of ocrelizumab. Mean with SEM are shown. P-values in bold are statistically significant. Differences in the cytokine levels were assessed by a linear mixed model and normal distribution was checked using a normal quantile plot of the conditional residuals of the model. Abbreviations: GM-CSF, granulocyte macrophage colony stimulating factor; IFN, interferon; IL, interleukin; IP-10, IFN-γ-induced protein 10; SEM, standard error of the mean; TNF-α, tumor necrosis factor alpha.

0.0141, data not shown). Thus, the concentrations of the pro-inflammatory cytokine IL-12p70 and anti-viral cytokine IFN-α2 were reduced in RRMS and PPMS patients after 12 M of ocrelizumab treatment.

4. Discussion

The B cell depletion therapy ocrelizumab is an effective treatment for RRMS and PPMS, but is also associated with an increased risk of infections [6,7,13,14,25]. Therefore, there is still a high need for detailed immune profiling after ocrelizumab treatment to better understand how B cell depleted MS patients can deal with life-threatening infections. In this study, we longitudinally examined the effect of ocrelizumab treatment on innate and adaptive immune cell populations and cytokine levels in a real-world cohort of RRMS and PPMS patients. High-dimensional flow cytometry revealed that circulating CD20⁺ B cells were successfully reduced after ocrelizumab treatment, both in absolute numbers and frequencies. Additionally, CD20⁺ T cell numbers were decreased in all patients. Within CD20⁻ immune cells, CD56ʰⁱ NK cells were reduced, whereas numbers of CD8⁺ T cells, monocytes and DCs were increased following ocrelizumab treatment. While overall B cell numbers were diminished, a shift in the residual B cell population was observed towards transitional B cells and activated, IgA⁺ antigen-experienced B cells (antibody-secreting cells, switched memory and double negative B cells). Extended interval dosing in two RRMS patients resulted in a repopulation of antigen-inexperienced naive B cells. Furthermore, plasma levels of the pro-inflammatory cytokine IL-12p70 and anti-viral cytokine IFN-α2 were reduced after 12 M of ocrelizumab treatment.

Our study confirmed the efficacy of ocrelizumab treatment as all RRMS patients and the majority of PPMS patients reached NEDA-3 after 1 year of treatment consistent with the results of clinical trials [6,7] and observational studies [18,19]. In contrast to the clinical trials, almost all patients in our cohort had been treated prior to ocrelizumab providing us a real-world cohort rather than a controlled dataset. While B cell depletion was observed in all PPMS patients who did not reach NEDA-3, our analysis did reveal an increased frequency of double negative B cells and elevated concentration of IFN-γ in these patients compared to PPMS patients who did reach NEDA-3 after 12 M of ocrelizumab. Increased frequencies of double negative B cells were already described in the peripheral blood and cerebrospinal fluid (CSF) of a proportion of MS patients [26,27]. These double negative B cells showed a pro-inflammatory phenotype and function suggesting their pathological role in MS pathogenesis [26], which could potentially explain the failure to reach NEDA-3 in PPMS patients with high frequencies of residual double negative B cells. While further validation in a larger patient cohort is warranted, this finding suggests the importance of analyzing B cell subset distribution in order to understand the clinical efficacy of ocrelizumab. This is consistent with observations in rheumatoid arthritis (RA), where the extent of B cell depletion was not predictive of therapy response, although differences in baseline plasmablast frequency were shown in non-responders [28].

In accordance with other studies, the absolute number of CD20⁺ T cells was significantly decreased after ocrelizumab treatment in both RRMS and PPMS patients [29,30]. CD20⁺ T cells have previously been found in the CSF of MS patients and were reported to have pro-

inflammatory functions [31,32]. Unlike other reports [29,33–36], no significant differences were found in the CD20⁻ T cell population of RRMS patients after ocrelizumab, while for PPMS patients an increase in the absolute CD8⁺ T cell numbers was observed after 12 M of ocrelizumab. This discrepancy may be due to differences in the study populations between studies. In our study, RRMS and PPMS patients were analyzed separately instead of being combined into one group [34–36]. Furthermore, the majority of MS patients in our real-world cohort were previously treated, mostly with only a short washout period, while changes in the CD4⁺ and CD8⁺ T cell populations were previously observed in treatment-naive RRMS [33] and PPMS patients [29]. In addition, we investigated the effect of one or two doses of ocrelizumab, while another study only reported an effect on CD8⁺ T cells after a third dose [34]. Another explanation could be that the T cells had already recovered after 6 M. This was demonstrated by a study in untreated RRMS and PPMS patients in which T cell levels were decreased directly after ocrelizumab infusion but quickly recovered after 3 M of ocrelizumab [30]. The reduced number of CD56ʰⁱ NK cells was in agreement with only one study, where the effect of one ocrelizumab dose was investigated in a cohort of treatment-naive PPMS patients [29]. In addition, we confirmed other reports in the increased absolute number of monocytes following ocrelizumab treatment, whereas the increased number of mDCs and pDCs was not in correspondence with literature [29,30]. The increase in antigen-presenting cells might compensate for the decrease in antigen-presenting B cells. To confirm this hypothesis, research should also focus on how B cell depletion therapy affects the function of the innate immunity. The differences in the distribution of the immune cell subsets suggest that the effect of ocrelizumab is patient dependent and highlight the importance of investigating the working mechanism of ocrelizumab in different cohorts.

The shift towards more transitional B cells and antibody-secreting cells within the residual B cell population is in agreement with another study on ocrelizumab [29]. Furthermore, an increased frequency of switched memory and double negative B cells within the residual B cell population was observed after rituximab treatment in MS patients [37] and for double negative B cells also in RA patients [38]. Additionally, we found that the residual B cells were more activated as indicated by the shift towards CD21⁻ cells (T1 transitional, CD21⁻ double negative, activated naive) as well as the increased frequency of CD86⁺ and CD80⁺ cells within the antibody-secreting cells, switched memory and double negative B cells. This was also observed after rituximab treatment as the majority of the residual switched memory and double negative B cells was CD21⁻ in RA patients [38], and an increased frequency of CD86⁺ B cells was observed in RRMS patients [39]. Furthermore, the majority of antigen-experienced cells were IgA⁺ class-switched. Previous research in rituximab treated RA patients showed increased levels of gut-derived IgA⁺ antibody-secreting cells [40]. In MS, gut-derived IgA⁺ antibody-secreting cells can migrate to the CNS and are assumed to have a regulatory function by secreting IL-10 [41,42]. Further analysis is needed to investigate if the residual IgA⁺ B cells observed post-ocrelizumab treatment are also regulatory, gut-derived cells. Our observations suggest that the remaining B cell population consists of repopulating transitional cells on one hand and on the other hand of activated, antigen-experienced cells, possibly less responsive to ocrelizumab, as was also hypothesized in rituximab studies [37,38]. However, the role of the residual B cells, whether regulatory or pro-inflammatory, in MS pathology remains unclear. Additionally, their increased activation state might compensate for the reduced B cell count in the protective immune responses against infections.

Increasing the time between two ocrelizumab doses could be beneficial for vaccination strategies by enabling repopulation of antigen-inexperienced T2 transitional and resting naive B cells, and reducing the frequency of residual CD86⁺ antigen-experienced cells. This is in line with a recent study that showed an increased repopulation of transitional, naive and regulatory B cells after extended interval dosing

compared to standard dosing schemes [43]. Several studies have shown in the context of COVID-19 that extended interval dosing does not affect the short-term disease activity [44–48]. However, more research on the long-term effect is warranted.

Cytokine analysis indicated reduced plasma levels of IL-12p70 and IFN-α2 after 12 M of ocrelizumab treatment in all MS patients. It is unclear whether the lower IL-12p70 concentration is due to B cell depletion or impaired monocyte and DC functioning. IFN-α2 is produced by the innate immune system in response to viral infections [49]. The reduction in IFN-α2 levels and the attenuated humoral immune response could explain the increased risk of severe infections such as COVID-19 in ocrelizumab treated MS patients [15,16]. Unlike other studies [29,30,50], we did not observe differences in the concentration of other pro-inflammatory cytokines following ocrelizumab treatment. This could be explained by variations in experimental set-up as intracellular cytokine staining on PBMCs revealed an increase in IL-6 and GM-CSF producing B cells in ocrelizumab treated PPMS patients [29]. Contradictory, ocrelizumab induced a decreased frequency of IL-6⁺ B cells in another study [50]. Multiplex analysis using serum instead of plasma also showed no significant differences in IL-6, TNF-α and IFN-γ levels after 6 M and 12 M of ocrelizumab [18]. Another study reported an increase in IL-6, TNF-α and IFN-γ levels in serum samples after 1 week of ocrelizumab that declined during follow-up [30]. Consequently, there remains a lack of consensus regarding the effect of ocrelizumab on cytokine levels. Moreover, our real-world cohort mainly consisted of previously treated patients and together with limited washout periods, baseline cytokine levels did not represent a naive inflammatory MS state. Another limitation of this study was the small sample size, particularly among patients with extended interval dosing, because this was a single-center study with patient dropout during the observation period.

Taken together, we investigated the effect of ocrelizumab treatment on the immune system in a real-world cohort of RRMS and PPMS patients over a 12 M period. High-dimensional flow cytometry revealed that not only the CD20⁺ cell populations were affected by ocrelizumab but also the number of CD56ʰⁱ NK cells, monocytes and DCs. The residual B cell population mainly consisted of repopulating transitional B cells and activated antigen-experienced cells, potentially less responsive to anti-CD20 therapy. Extended interval dosing in two RRMS patients suggested a repopulation of antigen-inexperienced cells. Future studies should examine the long-term clinical outcomes of these shifts in B cell subsets and their potential impact. With knowledge gained from this study, clinicians and researchers can better tailor therapeutic strategies to ensure optimal outcomes for RRMS and PPMS patients.

Author contributions

L.B., P.B., M.K., B.B., J.F. and V.S. were involved in the conceptualization of the study. S.J.T. was involved in the methodology by providing essential reagents and designing flow cytometry panel 1 for extended immunophenotyping. V.P. and B.V.M. were involved in the methodology by recruiting MS patients. V.P. also collected clinical data from MS patients. L.B., P.B. and D.S. acquired the data. L.B., P.B., D.S., A.C. and I.H. analyzed the data. L.B., P.B. and J.F. wrote the original draft of the manuscript and I.H., S.J.T., M.K., B.B. and V.S. reviewed and

edited the manuscript. All authors read and approved the final manuscript.

Declaration of competing interest

All authors have no conflict of interest to declare relevant to this article.

Data availability

Anonymized data not published within this article and supporting the findings of the study will be made available by request from any qualified investigator.

Acknowledgements

Appendix A. Supplementary data

Supplementary data to this article can be found online at https://doi.org/10.1016/j.clim.2024.109894.

References

[1] S. Klineova, F.D. Lublin, Clinical course of multiple sclerosis, Cold Spring Harb. Perspect. Med. 8 (9) (2018).
[2] B. Obermeier, R. Mentele, J. Malotka, J. Kellermann, T. Kümpfel, H. Wekerle, F. Lottspeich, R. Hohlfeld, K. Dornmair, Matching of oligoclonal immunoglobulin transcriptomes and proteomes of cerebrospinal fluid in multiple sclerosis, Nat. Med. 14 (6) (2008) 688–693.
[3] J. Fraussen, N. Claes, B. Van Wijmeersch, J. Van Horssen, P. Stinissen, R. Hupperts, V. Somers, B cells of multiple sclerosis patients induce autoreactive proinflammatory T cell responses, Clin. Immunol. 173 (2016) 124–132.
[4] M. Duddy, M. Niino, F. Adatia, S. Hebert, M. Freedman, H. Atkins, H.J. Kim, A. Bar-Or, Distinct effector cytokine profiles of memory and naive human B cell subsets and implication in multiple sclerosis, J. Immunol. 178 (10) (2007) 6092–6099.
[5] N. Claes, J. Fraussen, P. Stinissen, R. Hupperts, V. Somers, B cells are multifunctional players in multiple sclerosis pathogenesis: insights from therapeutic interventions, Front. Immunol. 6 (2015) 642.
[6] S.L. Hauser, A. Bar-Or, G. Comi, G. Giovannoni, H.P. Hartung, B. Hemmer, F. Lublin, X. Montalban, K.W. Rammohan, K. Selmaj, A. Traboulsee, J.S. Wolinsky, D.L. Arnold, G. Klingelschmitt, D. Masterman, P. Fontoura, S. Belachew, P. Chin, N. Mairon, H. Garren, L. Kappos, I. Opera, O.I.C. Investigators, Ocrelizumab versus interferon beta-1a in relapsing multiple sclerosis, N. Engl. J. Med. 376 (3) (2017) 221–234.
[7] X. Montalban, S.L. Hauser, L. Kappos, D.L. Arnold, A. Bar-Or, G. Comi, J. de Seze, G. Giovannoni, H.P. Hartung, B. Hemmer, F. Lublin, K.W. Rammohan, K. Selmaj, A. Traboulsee, A. Sauter, D. Masterman, P. Fontoura, S. Belachew, H. Garren, N. Mairon, P. Chin, J.S. Wolinsky, O.C. Investigators, Ocrelizumab versus placebo in primary progressive multiple sclerosis, N. Engl. J. Med. 376 (3) (2017) 209–220.
[8] F. Faustini, N. Sippl, R. Stålesen, K. Chemin, N. Dunn, A. Fogdell-Hahn, I. Gunnarsson, V. Malmström, Rituximab in systemic lupus erythematosus: transient effects on autoimmunity associated lymphocyte phenotypes and implications for immunogenicity, Front. Immunol. 13 (2022) 826152.
[9] P. Joly, M. Maho-Vaillant, C. Prost-Squarcioni, V. Hebert, E. Houivet, S. Calbo, F. Caillot, M.L. Golinski, B. Labeille, C. Picard-Dahan, C. Paul, M.A. Richard, J. D. Bouaziz, S. Duvert-Lehembre, P. Bernard, F. Caux, M. Alexandre, S. Ingen-Housz-Oro, P. Vabres, E. Delaporte, G. Quereux, A. Dupuy, S. Debarbieux, M. Avenel-Audran, M. D'Incan, C. Bedane, N. Bénéton, D. Jullien, N. Dupin, L. Misery, L. Machet, M. Beylot-Barry, O. Dereure, B. Sassolas, T. Vermeulin, J. Benichou, P. Musette, F.s.g.o.a.b.s. diseases, First-line rituximab combined with short-term prednisone versus prednisone alone for the treatment of pemphigus (Ritux 3): a prospective, multicentre, parallel-group, open-label randomised trial, Lancet 389 (10083) (2017) 2031–2040.
[10] J.H. Stone, P.A. Merkel, R. Spiera, P. Seo, C.A. Langford, G.S. Hoffman, C. G. Kallenberg, E.W. St Clair, A. Turkiewicz, N.K. Tchao, L. Webber, L. Ding, L. P. Sejismundo, K. Mieras, D. Weitzenkamp, D. Ikle, V. Seyfert-Margolis, M. Mueller, P. Brunetta, N.B. Allen, F.C. Fervenza, D. Geetha, K.A. Keogh, E. Y. Kissin, P.A. Monach, T. Peikert, C. Stegeman, S.R. Ytterberg, U. Specks, R.-I.R.

[10] Group, Rituximab versus cyclophosphamide for ANCA-associated vasculitis, N. Engl. J. Med. 363 (3) (2010) 221–232.
[11] M.J. Leandro, G. Cambridge, M.R. Ehrenstein, J.C. Edwards, Reconstitution of peripheral blood B cells after depletion with rituximab in patients with rheumatoid arthritis, Arthritis Rheum. 54 (2) (2006) 613–620.
[12] S.L. Hauser, A. Bar-Or, J.A. Cohen, G. Comi, J. Correale, P.K. Coyle, A.H. Cross, J. de Seze, D. Leppert, X. Montalban, K. Selmaj, H. Wiendl, C. Kerloeguen, R. Willi, B. Li, A. Kakarieka, D. Tomic, A. Goodyear, R. Pingili, D.A. Häring, K. Ramanathan, M. Merschhemke, L. Kappos, A.I.a.A.I.T. Groups, Ofatumumab versus teriflunomide in multiple sclerosis, N. Engl. J. Med. 383 (6) (2020) 546–557.
[13] M. Habek, D. Piskač, T. Gabelić, B. Barun, I. Adamec, M. Krbot Skorić, Hypogammaglobulinemia, infections and COVID-19 in people with multiple sclerosis treated with ocrelizumab, Mult. Scler. Relat. Disord. 62 (2022) 103798.
[14] N. Seery, S. Sharmin, V. Li, A.L. Nguyen, C. Meaton, R. Atvars, N. Taylor, K. Tunnell, J. Carey, M.P. Marriott, K.A. Buzzard, I. Roos, C. Dwyer, J. Baker, L. Taylor, K. Spriggs, T.J. Kilpatrick, T. Kalincik, M. Monif, Predicting infection risk in multiple sclerosis patients treated with ocrelizumab: a retrospective cohort study, CNS Drugs 35 (8) (2021) 907–918.
[15] A. Salter, R.J. Fox, S.D. Newsome, J. Halper, D.K.B. Li, P. Kanellis, K. Costello, B. Bebo, K. Rammohan, G.R. Cutter, A.H. Cross, Outcomes and risk factors associated with SARS-CoV-2 infection in a north American registry of patients with multiple sclerosis, JAMA Neurol. 78 (6) (2021) 699–708.
[16] S. Simpson-Yap, A. Pirmani, T. Kalincik, E. De Brouwer, L. Geys, T. Parciak, A. Helme, N. Rijke, J.A. Hillert, Y. Moreau, G. Edan, S. Sharmin, T. Spelman, R. McBurney, H. Schmidt, A.B. Bergmann, S. Braune, A. Stahmann, R. M. Middleton, A. Salter, B. Bebo, A. Van der Walt, H. Butzkueven, S. Ozakbas, C. Boz, R. Karabudak, R. Alroughani, J.I. Rojas, I.A. van der Mei, G. Sciascia do Olival, M. Magyari, R.N. Alonso, R.S. Nicholas, A.S. Chertcoff, A.Z. de Torres, G. Arrambide, N. Nag, A. Descamps, L. Costers, R. Dobson, A. Miller, P. Rodrigues, V. Prčkovska, G. Comi, L.M. Peeters, Updated results of the COVID-19 in MS global data sharing initiative: anti-CD20 and other risk factors associated with COVID-19 severity, Neurol. Neuroimmunol. Neuroinflamm. 9 (6) (2022).
[17] J.B. Smith, E.G. Gonzales, B.H. Li, A. Langer-Gould, Analysis of rituximab use, time between rituximab and SARS-CoV-2 vaccination, and COVID-19 hospitalization or death in patients with multiple sclerosis, JAMA Netw. Open 5 (12) (2022) e2248664.
[18] M. Boziki, C. Bakirtzis, S.A. Sintila, E. Kesidou, E. Gounari, A. Ioakimidou, V. Tsavdaridou, L. Skoura, A. Fylaktou, V. Nikolaidou, M. Stangou, I. Nikolaidis, V. Giantzi, E. Karafoulidou, P. Theotokis, N. Grigoriadis, Ocrelizumab in patients with active primary progressive multiple sclerosis: clinical outcomes and immune markers of treatment response, Cells 11 (12) (2022).
[19] M. Cellerino, G. Boffa, C. Lapucci, F. Tazza, E. Sbragia, E. Mancuso, N. Bruschi, S. Minguzzi, F. Ivaldi, I. Poirè, A. Laroni, G. Mancardi, E. Capello, A. Uccelli, G. Novi, M. Inglese, Predictors of ocrelizumab effectiveness in patients with multiple sclerosis, Neurotherapeutics 18 (4) (2021) 2579–2588.
[20] L. Linsen, K. Vanhees, E. Vanoppen, M. Ulenaers, S. Driessens, J. Penders, V. Somers, P. Stinissen, J.L. Rummens, Raising to the challenge: building a federated biobank to accelerate translational research-the university biobank Limburg, Front. Med. (Lausanne) 6 (2019) 224.
[21] A.J. Thompson, B.L. Banwell, F. Barkhof, W.M. Carroll, T. Coetzee, G. Comi, J. Correale, F. Fazekas, M. Filippi, M.S. Freedman, K. Fujihara, S.L. Galetta, H. P. Hartung, L. Kappos, F.D. Lublin, R.A. Marrie, A.E. Miller, D.H. Miller, X. Montalban, E.M. Mowry, P.S. Sorensen, M. Tintoré, A.L. Traboulsee, M. Trojano, B.M.J. Uitdehaag, S. Vukusic, E. Waubant, B.G. Weinshenker, S.C. Reingold, J. A. Cohen, Diagnosis of multiple sclerosis: 2017 revisions of the McDonald criteria, Lancet Neurol. 17 (2) (2018) 162–173.
[22] S. Van Gassen, B. Callebaut, M.J. Van Helden, B.N. Lambrecht, P. Demeester, T. Dhaene, Y. Saeys, FlowSOM: using self-organizing maps for visualization and interpretation of cytometry data, Cytometry A 87 (7) (2015) 636–645.
[23] L. Pandit, No evidence of disease activity (NEDA) in multiple sclerosis - shifting the goal posts, Ann. Indian Acad. Neurol. 22 (3) (2019) 261–263.
[24] Y. Saeys, S. Van Gassen, B.N. Lambrecht, Computational flow cytometry: helping to make sense of high-dimensional immunology data, Nat. Rev. Immunol. 16 (7) (2016) 449–462.
[25] J. Peters, E.E. Longbrake, Infection risk in a real-world cohort of patients treated with long-term B-cell depletion for autoimmune neurologic disease, Mult. Scler. Relat. Disord. 68 (2022) 104400.
[26] N. Claes, J. Fraussen, M. Vanheusden, N. Hellings, P. Stinissen, B. Van Wijmeersch, R. Hupperts, V. Somers, Age-associated B cells with proinflammatory characteristics are expanded in a proportion of multiple sclerosis patients, J. Immunol. 197 (12) (2016) 4576–4583.
[27] J. Fraussen, S. Marquez, K. Takata, L. Beckers, G. Montes Diaz, C. Zografou, B. Van Wijmeersch, L.M. Villar, K.C. O'Connor, S.H. Kleinstein, V. Somers, Phenotypic and Ig repertoire analyses indicate a common origin of IgD-CD27- double negative B cells in healthy individuals and multiple sclerosis patients, J. Immunol. 203 (6) (2019) 1650–1664.
[28] H.P. Brezinschek, F. Rainer, K. Brickmann, W.B. Graninger, B lymphocyte-typing for prediction of clinical response to rituximab, Arthritis Res. Ther. 14 (4) (2012) R161.
[29] J.I. Fernández-Velasco, J. Kuhle, E. Monreal, V. Meca-Lallana, J. Meca-Lallana, G. Izquierdo, F. Gascón-Giménez, S. Sainz de la Maza, P.E. Walo-Delgado, A. Maceski, E. Rodríguez-Martín, E. Roldán, N. Villarrubia, A. Saiz, Y. Blanco, P. Sánchez, E. Carreón-Guarnizo, Y. Aladro, L. Brieva, C. Íñiguez, I. González-Suárez, L.A. Rodríguez de Antonio, J. Masjuan, L. Costa-Frossard, L.M. Villar, Effect of ocrelizumab in blood leukocytes of patients with primary progressive MS, Neurol. Neuroimmunol. Neuroinflamm. 8 (2) (2021).

[30] K. Akgün, J. Behrens, D. Schriefer, T. Ziemssen, Acute effects of ocrelizumab infusion in multiple sclerosis patients, Int. J. Mol. Sci. 23 (22) (2022).

[31] E. Schuh, K. Berer, M. Mulazzani, K. Feil, I. Meinl, H. Lahm, M. Krane, R. Lange, K. Pfannes, M. Subklewe, R. Gürkov, M. Bradl, R. Hohlfeld, T. Kümpfel, E. Meinl, M. Krumbholz, Features of human CD3+CD20+ T cells, J. Immunol. 197 (4) (2016) 1111–1117.

[32] V.O. Boldrini, R.P.S. Quintiliano, L.S. Silva, A. Damasceno, L.M.B. Santos, A. S. Farias, Cytotoxic profile of CD3+CD20+ T cells in progressive multiple sclerosis, Mult. Scler. Relat. Disord. 52 (2021) 103013.

[33] A. Garcia, E. Dugast, S. Shah, J. Morille, C. Lebrun-Frenay, E. Thouvenot, J. De Sèze, E. Le Page, S. Vukusic, A. Maurousset, E. Berger, O. Casez, P. Labauge, A. Ruet, C. Raposo, F. Bakdache, R. Buffels, F. Le Frère, A. Nicot, S. Wiertlewski, P. A. Gourraud, L. Berthelot, D. Laplaud, Immune profiling reveals the T-cell effect of ocrelizumab in early relapsing-remitting multiple sclerosis, Neurol. Neuroimmunol. Neuroinflamm. 10 (3) (2023).

[34] N. Capasso, R. Palladino, V. Cerbone, A.L. Spiezia, B. Covelli, A. Fiore, R. Lanzillo, A. Carotenuto, M. Petracca, L. Stanziola, G. Scalia, V. Brescia Morra, M. Moccia, Ocrelizumab effect on humoral and cellular immunity in multiple sclerosis and its clinical correlates: a 3-year observational study, J. Neurol. 270 (1) (2023) 272–282.

[35] N. Capasso, A. Nozzolillo, G. Scalia, R. Lanzillo, A. Carotenuto, M. De Angelis, M. Petruzzo, F. Saccà, C.V. Russo, V. Brescia Morra, M. Moccia, Ocrelizumab depletes T-lymphocytes more than rituximab in multiple sclerosis, Mult. Scler. Relat. Disord. 49 (2021) 102802.

[36] D. Landi, A. Grimaldi, F. Bovis, M. Ponzano, R. Fantozzi, F. Buttari, E. Signoriello, G. Lus, M. Lucchini, M. Mirabella, M. Cellerino, M. Inglese, G. Cola, C.G. Nicoletti, G. Mataluni, D. Centonze, G.A. Marfia, Influence of previous disease-modifying drug exposure on T-lymphocyte dynamic in patients with multiple sclerosis treated with ocrelizumab, Neurol. Neuroimmunol. Neuroinflamm. 9 (3) (2022).

[37] A. Palanichamy, S. Jahn, D. Nickles, M. Derstine, A. Abounasr, S.L. Hauser, S. E. Baranzini, D. Leppert, H.C. von Büdingen, Rituximab efficiently depletes increased CD20-expressing T cells in multiple sclerosis patients, J. Immunol. 193 (2) (2014) 580–586.

[38] D.G. Adlowitz, J. Barnard, J.N. Biear, C. Cistrone, T. Owen, W. Wang, A. Palanichamy, E. Ezealah, D. Campbell, C. Wei, R.J. Looney, I. Sanz, J.H. Anolik, Expansion of activated peripheral blood memory B cells in rheumatoid arthritis, impact of B cell depletion therapy, and biomarkers of response, PLoS One 10 (6) (2015) e0128269.

[39] N. Nissimov, Z. Hajiyeva, S. Torke, K. Grondey, W. Brück, S. Häusser-Kinzel, M. S. Weber, B cells reappear less mature and more activated after their anti-CD20-mediated depletion in multiple sclerosis, Proc. Natl. Acad. Sci. U. S. A. 117 (41) (2020) 25690–25699.

[40] H.E. Mei, D. Frölich, C. Giesecke, C. Loddenkemper, K. Reiter, S. Schmidt, E. Feist, C. Daridon, H.P. Tony, A. Radbruch, T. Dörner, Steady-state generation of mucosal IgA+ plasmablasts is not abrogated by B-cell depletion therapy with rituximab, Blood 116 (24) (2010) 5181–5190.

[41] A.K. Pröbstel, X. Zhou, R. Baumann, S. Wischnewski, M. Kutza, O.L. Rojas, K. Sellrie, A. Bischof, K. Kim, A. Ramesh, R. Dandekar, A.L. Greenfield, R. D. Schubert, J.E. Bisanz, S. Vistnes, K. Khaleghi, J. Landefeld, G. Kirkish, F. Liesche-Starnecker, V. Ramaglia, S. Singh, E.B. Tran, P. Barba, K. Zorn, J. Oechtering, K. Forsberg, L.R. Shiow, R.G. Henry, J. Graves, B.A.C. Cree, S. L. Hauser, J. Kuhle, J.M. Gelfand, P.M. Andersen, J. Schlegel, P.J. Turnbaugh, P.

H. Seeberger, J.L. Gommerman, M.R. Wilson, L. Schirmer, S.E. Baranzini, Gut microbiota-specific IgA+ B cells traffic to the CNS in active multiple sclerosis, Sci. Immunol. 5 (53) (2020).

[42] O.L. Rojas, A.K. Pröbstel, E.A. Porfilio, A.A. Wang, M. Charabati, T. Sun, D.S. W. Lee, G. Galicia, V. Ramaglia, L.A. Ward, L.Y.T. Leung, G. Najafi, K. Khaleghi, B. Garcillán, A. Li, R. Besla, I. Naouar, E.Y. Cao, P. Chiaranunt, K. Burrows, H. G. Robinson, J.R. Allanach, J. Yam, H. Luck, D.J. Campbell, D. Allman, D. G. Brooks, M. Tomura, R. Baumann, S.S. Zamvil, A. Bar-Or, M.S. Horwitz, D. A. Winer, A. Mortha, F. Mackay, A. Prat, L.C. Osborne, C. Robbins, S.E. Baranzini, J.L. Gommerman, Recirculating intestinal IgA-producing cells regulate neuroinflammation via IL-10, Cell 176 (3) (2019) 610–624, e18.

[43] C. Rodriguez-Mogeda, Z.Y.G.J. van Lierop, S.M.A. van der Pol, L. Coenen, L. Hogenboom, A. Kamermans, E. Rodriguez, J. van Horssen, Z.L.E. van Kempen, B. M.J. Uitdehaag, C.E. Teunissen, M.E. Witte, J. Killestein, H.E. de Vries, Extended interval dosing of ocrelizumab modifies the repopulation of B cells without altering the clinical efficacy in multiple sclerosis, J. Neuroinflammation 20 (1) (2023) 215.

[44] L. Rolfes, M. Pawlitzki, S. Pfeuffer, C. Nelke, A. Lux, R. Pul, C. Kleinschnitz, K. Kleinschnitz, R. Rogall, K. Pape, S. Bittner, F. Zipp, C. Warnke, Y. Goereci, M. Schroeter, J. Ingwersen, O. Aktas, L. Klotz, T. Ruck, H. Wiendl, S.G. Meuth, Ocrelizumab extended interval dosing in multiple sclerosis in times of COVID-19, Neurol. Neuroimmunol. Neuroinflamm. 8 (5) (2021).

[45] S. Guerrieri, C. Bucca, A. Nozzolillo, A. Genchi, C. Zanetta, I. Cetta, G. Rugarli, I. Gattuso, M. Azzimonti, M.A. Rocca, L. Moiola, M. Filippi, S.M.S. Group, Ocrelizumab extended-interval dosing in multiple sclerosis during SARS-CoV-2 pandemic: a real-world experience, Eur. J. Neurol. 30 (9) (2023) 2859–2864.

[46] Z.Y. van Lierop, A.A. Toorop, W.J. van Ballegoij, T.B. Olde Dubbelink, E.M. Strijbis, B.A. de Jong, B.W. van Oosten, B. Moraal, C.E. Teunissen, B.M. Uitdehaag, J. Killestein, Z.L.V. Kempen, Personalized B-cell tailored dosing of ocrelizumab in patients with multiple sclerosis during the COVID-19 pandemic, Mult. Scler. 28 (7) (2022) 1121–1125.

[47] A. Zanghì, C. Avolio, E. Signoriello, G. Abbadessa, M. Cellerino, D. Ferraro, C. Messina, S. Barone, G. Callari, E. Tsantes, P. Sola, P. Valentino, F. Granella, F. Patti, G. Lus, S. Bonavita, M. Inglese, E. D'Amico, Is it time for ocrelizumab extended interval dosing in relapsing remitting MS? Evidence from an Italian multicenter experience during the COVID-19 pandemic, Neurotherapeutics 19 (5) (2022) 1535–1545.

[48] R. Claverie, M. Perriguey, A. Rico, C. Boutiere, S. Demortiere, P. Durozard, F. Hilezian, C. Dubrou, F. Vely, J. Pelletier, B. Audoin, A. Maarouf, Efficacy of rituximab outlasts B-cell repopulation in multiple sclerosis: time to rethink dosing? Neurol. Neuroimmunol. Neuroinflamm. 10 (5) (2023).

[49] L. Yang, J. Wang, P. Hui, T.O. Yarovinsky, S. Badeti, K. Pham, C. Liu, Potential role of IFN-α in COVID-19 patients and its underlying treatment options, Appl. Microbiol. Biotechnol. 105 (10) (2021) 4005–4015.

[50] K. Shinoda, R. Li, A. Rezk, I. Mexhitaj, K.R. Patterson, M. Kakara, L. Zuroff, J. L. Bennett, H.C. von Büdingen, R. Carruthers, K.R. Edwards, R. Fallis, P. S. Giacomini, B.M. Greenberg, D.A. Hafler, C. Ionete, U.W. Kaunzner, C.B. Lock, E. E. Longbrake, G. Pardo, F. Piehl, M.S. Weber, T. Ziemssen, D. Jacobs, J.M. Gelfand, A.H. Cross, B. Cameron, B. Musch, R.C. Winger, X. Jia, C.T. Harp, H. Herman, A. Bar-Or, Differential effects of anti-CD20 therapy on CD4 and CD8 T cells and implication of CD20-expressing CD8 T cells in MS disease activity, Proc. Natl. Acad. Sci. U. S. A. 120 (3) (2023) e2207291120.